Modeling and Analysis of a Fast Charging Station and Evaluation of Service Quality for Electric Vehicles

Emin Ucer, *Student Member, IEEE,* Işıl Koyuncu, Mithat C. Kisacikoglu, *Member, IEEE,* Mesut Yavuz, Andrew Meintz, and Clément Rames

***Abstract*—The deployment of public charging infrastructure networks has been a major factor in enabling electric vehicle (EV) technology transition, and must continue to support the adoption of this technology. DC fast charging (DCFC) increases customer convenience by lowering charging time, enables long-distance EV travel, and could allow the electrification of high-mileage fleets. Yet, high capital costs and uneven power demand have been major challenges to the widespread deployment of DCFC stations. There is a need to better understand DCFC stations' loading and customer service quality. Furthermore, the relationship between the initial investment decision on building certain number of ports and customer satisfaction should be quantified. This study aims to analyze these aspects using one million vehicle-days of travel data within the Columbus, OH, region. Monte Carlo analysis is carried out in three types of areas - urban, suburban, and rural- to quantify the effect of uncertain parameters on DCFC station loading and service quality. Additional simulations based on a homogeneous vehicle population are carried out, and closed-form equations are derived therefrom to estimate charging duration and waiting time in the queue. Optimization of DCFC station design is also addressed through the number and capacity of ports.**

***Index Terms*—Electric vehicles, DC fast chargers, optimization, modeling, queueing**

NOMENCLATURE

n	Number of DCFC ports
p	Power rating (capacity) of each port [kW]
P	Total power rating of the station [kW] (e.g. $P = np$)
δ	Arrival SOC of each vehicle (%)
d	Energy demand of each vehicle [kWh]
t_c	Charging duration of each vehicle [minutes]
W_q	Mean waiting time in the queue before charging [minutes]
s	Set-up time between two subsequent vehicles to be charged at the same port [minutes]

M. C. Kisacikoglu is with the Department of Electrical and Computer Engineering, University of Alabama, Tuscaloosa, AL, 35487 USA Phone: (205)-348-0219, e-mail: mkisacik@ua.edu

E. Ucer is with Dept. of Electrical and Computer Engineering, University of Alabama, Tuscaloosa, AL; I. Koyuncu and M. Yavuz are with Dept. of Information Systems, Statistics and Management Science, University of Alabama, Tuscaloosa, AL; A. Meintz and C. Rames are with National Renewable Energy Laboratory (NREL), Golden, CO.

The preliminary version of this work has been presented at IEEE Transportation Electrification Conference and Expo, June 13-15 2018, Long Beach, CA. This work was supported by the U.S. Dept. of Energy (DOE) under Contract No. DE-AC36-08GO28308 with NREL. This report and the work described to develop the DCFC model were sponsored by the U.S. DOE Vehicle Technologies Office under the Systems and Modeling for Accelerated Research in Transportation (SMART) Mobility Laboratory Consortium, an initiative of the Energy Efficient Mobility Systems (EEMS) Program.

I. INTRODUCTION

The electric vehicle (EV) market is taking off, with over 500k EVs on the road in the United States and over 2M globally. Although EVs are becoming more popular, the issues that prevent their mass penetration such as limited infrastructure are still present. Replacement of traditional internal combustion engine vehicles by EVs goes hand-in-hand with the mass deployment of reliable and fast charging infrastructure.

There are two types of EV charging methods: (i) on-board charger for AC grid connection which can be single-phase Level 1 (L1) and Level 2 (L2) as defined in SAE J1772, and three-phase AC charging as defined in SAE J3068 (work in progress); and (ii) DC fast charging (DCFC) as defined in SAE J1772-Combo/CHAdeMO standards. L1 and L2 are mostly located at residential and public/workplace charging premises. These stations do not include a power electronics converter but rather utilize the vehicle's on-board charger which is rated at low power levels (typically less than 19.2 kW) [1]. On the other hand, DCFC stations operate at high power DC voltage and use an off-board AC-DC converter. Thus, they provide much higher charging power level compared to L1 and L2.

There are several issues that should be addressed for the wide-spread usage of DCFC stations: their locations, operation costs, and how to evaluate the service quality for the customer [2]. DCFC geographic location has to be close to where it is needed and should ensure relatively high mobility of EVs [2]. Berjoza and Jurgena [2] proposed an algorithm that determines metrics like the availability ratio for charging stations. Zenginis et al. [3] describe a novel queuing model where the customers' mean waiting time is computed by considering the available charging outlets, arrival times, and charging needs of various EVs. Quality of service (QoS) is measured by waiting time of the customers in the queue prior to charging their EVs.

Fan et al. [4] studies the impact of the requested state of charge (SOC) of EVs on charging times and proposes an operation analysis of fast charging stations where operators can set a limit on the requested SOCs to obtain maximized revenue. Yunus et al. [5] investigated the impact of DCFC stations on distribution transformer loading using stochastic EV mobility parameters. System bus voltage profiles are also analyzed using DigSILENT PowerFactory. Akhavan-Rezai et al. [6] extracted mobility models from a national survey in Canada and used them to compare normal and DCFC stations in terms of their impact on voltage violations, power losses, and line loading.

Yang et al. [7] explores the optimal sizing problem of DCFC

stations. EV charging demand is calculated based on random generation of EV mobility statistics. Then, a queuing model is developed, and an optimization algorithm is run considering service quality and limitations of the power network. Compared to our study, the generated data set does not rely on real field data, and it does not implement any charge acceptance curve which is very limiting in the evaluation of service quality. [8] proposes an estimation method based on Markov arrival process for stochastic modeling of charging stations. They essentially aim to determine the required number of charge ports in a station to keep the probability of waiting below a pre-defined threshold. They use the number of arriving vehicles during a fixed time slot and service time distributions as inputs. However, this study does not fully describe important details such as vehicle type, charge acceptance, station location, and port capacity, but rather uses generic modeling.

Design and operational management of DCFC stations play a crucial role in meeting the requirements for high QoS. Metrics such as the average waiting time in queue (W_q) or average charging duration (t_c) depend mostly on DCFC design parameters (e.g. port number (n), total power rating (P), and individual port capacity (p)). Stations with lower waiting and charging times will attract more customers. Similarly, station design that gives the best QoS with minimum investment is desired by the station operator. These suggest that an analysis building a relationship between the total installation&operation costs and customer satisfaction have the potential to increase the total station revenue.

The National Renewable Energy Laboratory (NREL) together with the California Energy Commission (CEC) developed the Electric Vehicle Infrastructure Projection Tool (EVI-Pro) to estimate regional requirements for charging infrastructure to support consumer adoption of EVs [9], [10]. EVI-Pro utilizes EV market and real-world travel data to estimate future requirements for home, workplace, and public charging infrastructure [9], [10]. In this study, one million vehicle-days of travel from the Columbus, OH, region – the winner of the U.S. Department of Transportation's Smart City award [11] – were simulated in EVI-Pro to generate about 23,000 DCFC events. A lite version of this tool is publicly available at [12].

This study develops tools for and analyzes DCFC operation to minimize the costs while ensuring high customer satisfaction. We further present DCFC power consumption based on data provided by EVI-Pro. The model generates instantaneous and 15-minute average active power consumption to report peak demand consumption for a given system. To analyze the results of the simulation model, the present paper utilizes the queueing theory, data analytics and optimization. Queueing theory is helpful in estimating waiting times, which are directly related to customer satisfaction and QoS. We focus on a homogeneous vehicle population in our analysis, and supplement queueing theory approximation with data analytics to obtain a reliable closed-form expression of waiting time. We then optimize the power and number of ports of the DCFC station to simultaneously minimize cost and waiting time. The focus of the present paper is at the macro level; whereas the existing literature focuses on operational scheduling [13] or combines station design with location selection [14], [15].

The overview of the DCFC system operation is summarized in Fig. 1. An EV arrives at the DCFC station and waits for a specific time if there is a queue at the station. Then, when it is the EV's turn, the station charges the EV's battery based on its *initial SOC, energy demand, and available power capacity of the charging port.*

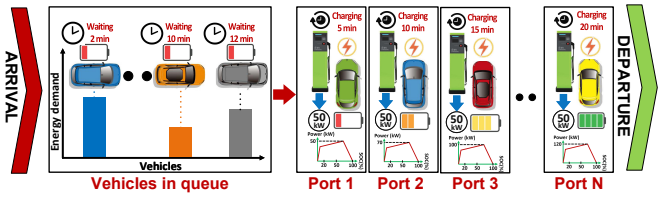

Figure 1: The overview of the DCFC model developed in this study.

Our contributions in this paper can be summarized as follows:

- A novel DCFC station model is developed as a tool to generate the charging and queuing statistics of any station for any given vehicle/customer data.
- The model is developed using highly-cleansed field mobility data and experimental EV DCFC power vs. SOC curves.
- Statistical Monte Carlo (MC) results comparing three station options suited for three different locations in terms of port numbers, and total power capacities are presented.
- The impact of station parameters on the QoS is clearly presented under the light of real field mobility data.
- An optimization algorithm is developed to further analyze the selection of port number and capacity that ensures minimum queuing times and initial investment requirement. This analysis sheds light on the difficult task of designing DCFC for a specific location QoS requirement.

The organization of the paper is as follows. Section II presents the methods of data collection from EVI-Pro. Section III describes the development of the DCFC station model and presents the statistical MC simulation results. Section IV is concerned with the mathematical analysis on DCFC operation to estimate average charging time, queuing time, and total station cost. Section V explains the optimal decision making to meet station requirements, and finally, Section VI concludes the study.

II. Data Collection Methodology and EVI-Pro Model

EVI-Pro anticipates spatially and temporally resolved consumer charging demand while capturing variations with respect to residents of single-unit dwellings (SUDs) and multi-unit dwellings (MUDs), weekday/weekend travel behavior, and regional differences in travel patterns and vehicle adoption. To identify the optimal charging strategy, individual travel days from a travel data set (originally completed using a conventional gasoline vehicle) are simulated in EVI-Pro under different assumptions for charging infrastructure availability. The EVI-Pro model is designed to model regular, everyday travel demand as represented in travel surveys and individual drivers' GPS datasets. It does not account for the occasional long distance road trip that would require on-route charging as it is inherently a different paradigm compared to everyday charging. Therefore, this paper examines the demand for "destination" or "community" DC Fast Chargers as opposed to "highway rest area" type stations.

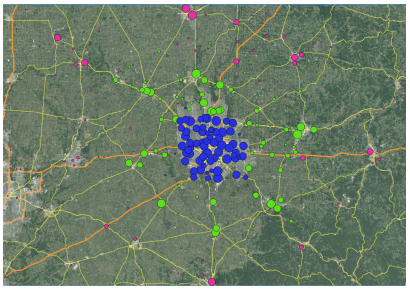

Figure 2: Map of station locations and charging events in Colombus, OH (Blue: urban, green: suburban, magenta: rural).

The modeled vehicle fleet consists of both plug-in hybrid (PHEVs) and battery electric vehicles (BEVs), but only BEVs are eligible to use DCFC stations. The default charging behavior is "home-dominant," meaning that consumers prefer to charge at their residence, then at their workplace, and finally in public locations. This charging demand simulation generates a set of charging sessions required to satisfy the travel patterns displayed in the data in a way that maximizes electric miles traveled and minimizes operational cost. These charging sessions are then post-processed spatially and temporally to output electric vehicle supply equipment (EVSE) requirements and station utilization for the Columbus region. More detail on this methodology can be found in [16].

EVI-Pro relies on real-world travel data to simulate EV charging demand. A large, commercial data set was procured from INRIX [17], consisting of GPS travel trajectories (mode imputed as driving trips by INRIX) that intersected the Columbus, OH, region in 2016. Each trajectory features trip-level data such as start/end times and GPS coordinates (including origins, destinations, and intermediate way points). The full data set was down selected to include only light-duty consumer vehicle GPS data collected from mobile/cellular devices. A thorough data cleansing routine was applied to ensure the integrity of travel days simulated in EVI-Pro. The cleansed input data set includes approximately 1.02 million full travel days, 3.71 million trips, and 30.6 million miles of driving.

The results of these simulations show that the majority of charging required to satisfy travel needs of drivers from the INRIX data set can be accommodated with residential charging. However, some DCFC is required to accommodate high vehicle miles traveled (VMT), short dwell time travel days. The simulation generated about 23,600 DCFC events across the Columbus region, with the highest density (just over half of all events) occurring in Franklin County, 30% occurring in the six neighboring counties, and the remaining 20% scattered across the rest of Ohio and the Midwest. These charging events are clustered into 400 DCFC stations, flagged as urban (Franklin County), suburban (six neighboring counties), and rural (outside of the Columbus metro area). The map of all stations are shown in Fig. 2. The size of the circles is proportional to the number of charging sessions, and the colors represent the three zones.

The number of DCFC charge events is determined in EVI-Pro by the daily travel schedule of simulated vehicles. DCFC is modeled as being the most expensive charging option, so drivers will only choose it if residential, workplace or public AC slow charging does not enable them to satisfy their travel demand. DCFC charge events are then aggregated into 400 stations by clustering them spatially to create "hot-spots", as opposed to point locations. Actual land use is currently not taken into account by the siting algorithm: as a result, there may be architectural or environmental constraints on station siting.

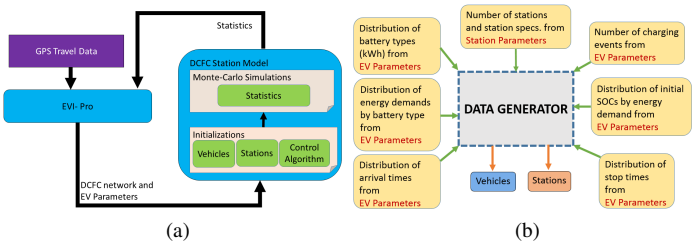

Figure 3: Structure of the (a) DCFC station model and EVI-Pro interaction and (b) data generation.

III. DCFC Station Load Model and Simulation Test Study

A. DCFC Station Modeling

Fig. 3a shows the structure of the interaction between the developed DCFC station model and EVI-Pro. EVI-Pro provides the necessary input data and stochastic mobility parameter distributions to the DCFC station model which in turn generates vehicle charging events and stations. The input data provided by EVI-Pro can be divided into three categories: (i) station parameters, (ii) vehicle parameters, and (iii) station use parameters.

Station parameters include number of stations, their capacities, number of ports, and port capacities. Vehicle parameters define vehicle types, battery sizes, maximum charging powers, and charge acceptance curves. The data also provide several distributions for vehicle types, arrival times, energy demands, and initial SOCs along with number of charging events at each station. A brief overview of the variable generation process is shown in Fig. 3b.

In order to understand the design criteria for a DCFC station, it is necessary to develop the likelihood of all possible outcomes and the risks these represent. The MC analysis is an effective tool for this purpose. It provides possible outcomes and also their associated probabilities bringing a broader view of what might happen. For this purpose, we utilized MC analysis by running 10 monthly simulations with the same input data. At each run, vehicle related parameters such as time of arrival, energy demand, initial SOC, etc. are randomly regenerated from the associated probability density functions (PDFs) as shown in Fig. 3b. During the simulations, vehicles arrive at the corresponding stations, wait in the queue (if there is not any available port), are plugged in, and then charged according to their charge acceptance curves. They depart after their energy demand is met, and a new vehicle from the queue is plugged into an available port.

B. Charge Acceptance Curves

The charge acceptance curves for the vehicle types are given in Fig. 4a. This figure shows how the charging power of vehicle batteries vary as a function of battery SOC. The curves for each vehicle type were developed based on DCFC data acquired from a 2012 Nissan LEAF [18]. This charging power data are collected after a full vehicle thermal soak to allow

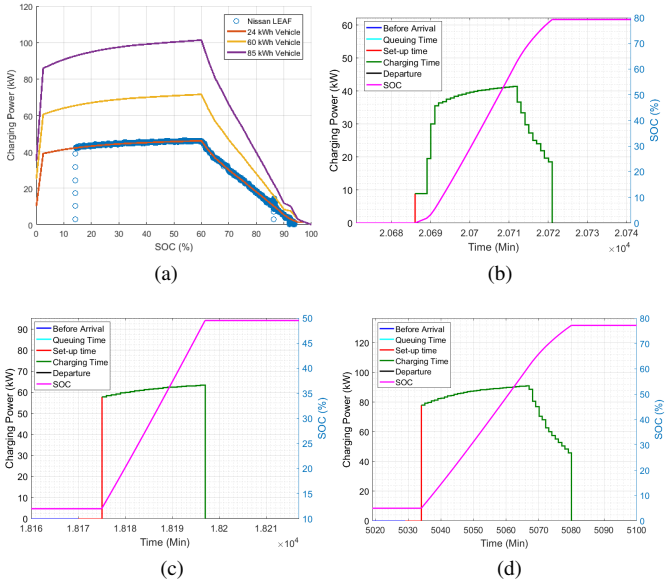

Figure 4: (a) Charge acceptance curves for three vehicle types with Nissan LEAF fast charging data, and (b) charging profile results of a 24 kWh, (c) 60 kWh, and (d) 85 kWh electric vehicle.

the battery to reach 25°C. The vehicle data are included in Fig. 4 and are for a charge from about 15% to 90% SOC. A curve-fit method is used to define the charge acceptance curve at intervals of 2.5% SOC for the 24 kWh vehicle type. The remaining charge acceptance curves are determined assuming a cell-level charge power decrease of 60% in the power-to-energy (P-E) ratio that is then scaled for the larger capacity 60 kWh and 85 kWh vehicle types. The decrease in P-E is used to account for the use of more energy dense cells in the production of longer range vehicles [19], [20].

These charge acceptance curves are used by the DCFC model to limit the charge power to the charging vehicles based on their SOC throughout the fast charge. Thermal and time-dependent charge diffusion limitations on charging power have not been accounted for in this model. The charge data from the Nissan LEAF demonstrate a simplified constant-current (CC) charging method up to 60% SOC and a then constant-voltage (CV) methodology to higher SOCs. While the SOC transition to constant-voltage may vary depending on battery chemistry and other more aggressive charging methods have been proposed [21] [22], this approach provides an approximation of the battery limitations on charging power.

C. Simulation Test Set-up

All the simulation parameters used in this study are listed in Table I. The justifications for the selection of parameters pertaining to vehicles and stations are explained as follows. We simulated three stations which characterize the three typical station configurations found today. The first station type, located in the urban core, has 12 ports and a total capacity of 1,800 kW, to respond to high demand. The second station type, located in suburban areas, has 4 ports and a total capacity of 600 kW. Finally, the third station type corresponds to a rural station with only one 50 kW port, which primarily serves to provide network coverage – i.e. a safety net – to BEV drivers traveling outside the city. The number of plugs for each station type was determined by averaging the number of plugs per station simulated in each zone (urban, suburban and rural, respectively).

Table I: Simulation, station, and vehicle parameters used in this study.

Station parameters			
	[1] Urban	[2] Suburban	[3] Rural
Number of ports	12	4	1
Station capacity [kW]	1800	600	50
Port capacity [kW]	150	150	50
Vehicle parameters			
	EV-1	EV-2	EV-3
Battery size [kWh]	24	60	85
Max. SOC limit [%]	80	80	80
Probability Distributions:			
Urban	0.8900	0.0503	0.0598
Suburban	0.8513	0.0691	0.0796
Rural	0.6403	0.1675	0.1922
Simulation parameters			
Total number of MC Simulations: 10			
Single simulation duration: 4 weeks (1-min resolution)			

The probability distributions for each EV type are determined by EVI-Pro based on the frequency at which each vehicle type utilizes DCFC stations in urban, suburban and rural settings. The DCFC network, regardless of station type, is primarily utilized by short range EVs whose daily driving distance can often exceed their range. 24 kWh EV owners residing in the urban core will be less inclined to drive to the farther outskirts of the city due to their limited range. Conversely, 85 kWh EV can complete longer trips and will utilize the rural DCFC network more frequently. When evaluating the impact of probability distributions to the model outputs, one should consider that charge acceptance rate increases with increased capacity EVs. This provides faster charge speeds when the port capacity is higher than the vehicle demand (i.e. in urban and suburban stations). However, the energy demand also increases with increased capacity EVs. In this study, we develop a methodological approach to factor in all the possible causes impacting the user experience at the DCFC station.

To demonstrate how a charging event takes place, the charging profiles of three different types of vehicles (with 24, 60, and 85 kWh battery sizes) are presented in Figs. 4b–4d, respectively. The vehicles are randomly selected out of approximately 23,000 charging events. In these figures, one can observe when the vehicles arrived at the stations, whether or not they had to wait in a queue (none of them entered the queue in the presented cases), its set-up time (selected as 5-min), and when its charging started. Further, one can observe how EVs' charging power changed over time as a result of charge acceptance rate, how their SOC changed, and when they finished with charging and departed.

The charge acceptance curves play a role in the total time EVs spend at the charging station. The main impact to the results are a function of the arrival SOC and the required energy demanded for each charge event. If the charge stays in the lower CC range of the chosen curves, it will have a minimal impact on the charge duration as seen in Fig. 5(b). However, as seen in Figs. 5(a) and (c), the rate of charge can reduce at the end of the charge (CV range). The charge

Table II: Important statistical results of MC simulations.

	Station Details	Station 1	Station 2	Station 3
	Station port count	12	4	1
	Station power capacity (kW)	1800	600	50
	Monthly charging events	3976	896	308
Charging Power	Aver. demand power (kW)	136.26	55.19	36.59
	Max. demand power (kW)	606.58	279.83	50
Charging Duration	Max. charging dur. (min)	54	54	91
	Aver. charging dur. (min)	20.73	21.73	35.14
	Min. charging dur. (min)	8	8	8
Queuing	Max. queuing dur. (min)	12	30	276
	Aver. queuing dur. (min)	0.04	0.25	30.14
	Max. queue length (# EV)	5	5	7
	Aver. queue length (# EV)	0.004	0.006	0.230
Port Utilization	Max. port util. (# ports)	12	4	1
	Aver. port util. (%)	30.8	39	100

acceptance rate will depend most dramatically on how a manufacturer develops the battery management system when trying to balance battery life constraints against both battery temperature and SOC.

We leave it for future work to examine in detail how these decisions will impact the queuing of a station and design decisions around the built infrastructure for a station. Our approach is to use the MC simulations that randomly assigns incoming SOC and required energy for these curves based on the EVI-Pro statistics explained above. Therefore, we believe we have bounded the problem appropriately and removed some of the impact of the chosen curves.

D. Simulation Results and Discussions

The simulations were run with the parameters defined above for a station design in each region using the average number of charge events of the stations in the respective region. Table II gives the statistical results of all MC simulations for each station. Four criteria have been chosen for analysis and comparison: 15-min average power consumption of the stations (termed as "demand power" in this study), charging duration statistics at each station, queuing statistics (queuing duration and queue length), and port usage. Table II can help draw important conclusions regarding the load profile, QoS, and effective use of available power at the station. As an example, an increase in average and peak demand power and a decrease in the queuing durations can be noted from station 3 to station 1 due to increased power capacities and port numbers. Further, maximum power consumption of station 1 is almost a third of the station total capacity. However, the same station experiences a maximum queuing duration as high as 12 min.

Demand charges can be as high as 90% of electricity costs of a DCFC station according to a recent report [23]. Therefore, demand power consumption of different DCFC station types are explained using box plots. Fig. 5 shows the box plots of demand power consumption of the stations for each day after 10 MC simulations. Bottom and top lines of each box represent 25th and 75th percentile of all samples, respectively. Straight lines in each box refer to median of all samples. Maximum limit of the dotted lines ($\top$) cover the 99.3%, and the remaining red outliers (+) fall into 0.7% of all samples.

Even though the total capacities of stations 1 and 2 are 1,800 kW and 600 kW, respectively, 75th percentile of all power consumptions fall well below their rated capacity with the outlier events below half of the rated power. The peak demand power for station 1 designated by the outliers is

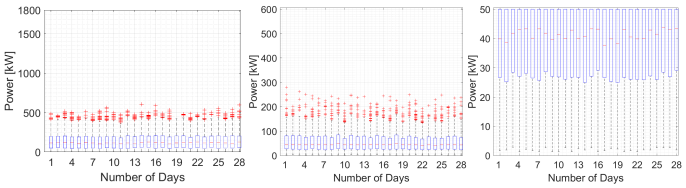

(a) (b) (c)

Figure 5: Demand power boxplots of stations (a) #1, (b) #2, and (c) #3.

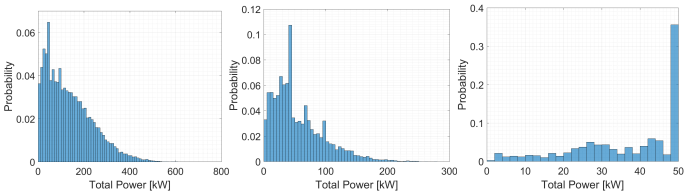

(a) (b) (c)

Figure 6: Demand power probability histograms of stations (a) #1, (b) #2, and (c) #3 (No EV case excluded).

around one-third of the station's rated capacity. This ratio is a little higher for station 2, indicating that the capacity of station 2 is more effectively used. Station 3, on the other hand, uses all of its capacity every day since it has only one port. This means that either or both a capacity increase and port count increase for this station should be considered.

Fig. 6 shows the probability histograms of the demand power consumption for all time at each station for 10 MC simulations. These figures show the likelihoods of total power consumptions that the stations will have to handle. As seen, the figures are consistent with the statistical results presented in Table II. Fig. 7 corresponds to the percent of station port utilization. "0 port" indicates the times when no EVs are present at the station. This figure reveals that 70% of the time, the ports of station 3 are not utilized. The percentages in the figure add up to 100% for each station corresponding to 24h horizon.

The queue at the station is another important parameter that results in extra waiting times and decreases QoS. The average and maximum queue length and queuing durations among all MC simulations for each station in a month were already given in Table II. Fig. 8 shows the probability of queuing durations at each station for the customers that happened to wait in the queue excluding zero waiting times. This provides better information on the queuing time spectrum. Further, the probabilities of waiting in different time intervals in a day are also calculated. The results are presented for different

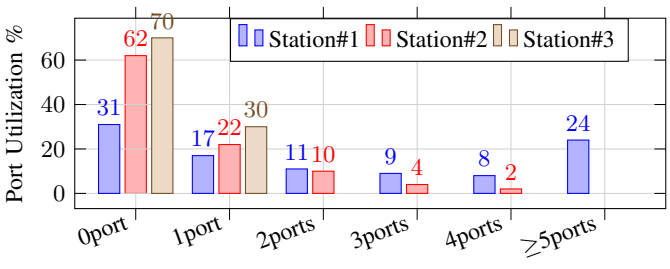

Figure 7: Port utilization of each station.

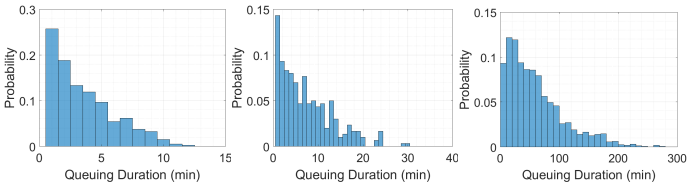

(a) (b) (c)

Figure 8: Queuing duration probabilities for stations (a) #1, (b) #2, and (c) #3. (zero queuing time excluded)

waiting times as a probability chart in Table III. It shows the probability of how long a user will wait in the queue at each station at any time of the day. As the queue length increases, the waiting times will increase and QoS will decrease. Since Station 1 offers charging at higher powers and has more ports, it is very unlikely to wait more than 10 min at this station. The worst case scenario happens for Station 3 where the probability of waiting more than 25 min in the queue between 12:00-14:00 is 37%. This also follows the statistical results in Table II that show the average waiting duration for Station 3 is 30 min. This is definitely not a reasonable risk for the station operator since it clearly loses potential customers to other stations. To overcome this problem, either the power capacity of the available port/station or installing an additional port should be considered.

To make the best decision in selecting the DCFC design parameters and providing a satisfactory QoS to customer, we will develop a mathematical formulation between the aforementioned parameters in the next section.

IV. Analysis to Estimate Average Charging Time, Queuing Time, and Total Cost

In this section, we use the queueing theory and analytics to approximate the customer satisfaction aspect of DCFC stations. The mathematical functions derived in this section serve as the building blocks of our optimization model in the next section.

In the preceding simulations, three different stations with three distinct sets of characteristics were used. In the following, we use a new station and [controllably] vary two of its critical characteristics for optimization.

For sake of simplicity, consider a station serving a homogeneous population of vehicles with 60 kWh battery capacity, i.e., type 2 vehicle in Section III. The charge acceptance curve (Fig. 4a) indicates that the maximum power needed by this vehicle is approximately 72 kW at 60% SOC. Investment costs depend on port capacity (p), hence it is suboptimal to set p higher than the maximum that can be utilized by the vehicles. However, it can be beneficial to strategically install lower-capacity ports to reduce investment costs. To investigate the effect of lower port capacity, we experiment with $p \in \{48, 60, 72\}$. Note that our analysis can be generalized to heterogeneous vehicle populations. Also note that installing higher-capacity ports than currently needed could be considered under speculative motives (such as vehicles with larger battery capacity utilizing the station in the future), which are excluded from this analysis.

Another design characteristic that directly affects costs is the number of ports (n). In the following, we show the results of a full-factorial experiment with two parameters ($n \in \{9, 10, 11, 12\}$ and $p \in \{48, 60, 72\}$) to see the effects of these two key station design parameters on customer satisfaction. The 12 combinations (of n and p) were simulated 10 times using the DCFC station model developed in Section III-A. In each run, 142 vehicles were populated per day, for 28 days. Consequently, there were $142 \times 28 \times 10 \times 12 = 477,120$ vehicles in the entire experiment. Some of our analyses are based on all 477,120 vehicles, whereas some others on the averages observed for each of the four n values and/or three p values.

All our analyses are conducted using the SAS 9.4 software package [24]. We rely on the p-value statistical measure where applicable. More specifically, we conduct regression analysis to predict a dependent variable and use the p-value to conclude on the strength of the hypothesized relationship between a set of independent variables and the dependent variable. The p-value values less than 0.01 are interpreted to show overwhelming evidence for the relationship [25, p. 397]. In interpreting regression analysis results, we also rely on the coefficient of determination (r^2), which is the fraction of variability in the dependent variable explained by using the estimated regression equation. Threshold r^2 values acceptable to conclude strong regression vary by application [25, p. 616]. In our case, we look for $r^2 \geq 0.90$. In building our regression models, we adopted the stepwise regression approach [25, p. 784], which is available in the SAS 9.4 package.

A. Estimating the charging duration

For a particular vehicle, charging duration is a function of port power, arrival SOC, and energy demand, i.e., $t_c = F(p, \delta, d)$. Charging duration is expected to be inversely related to p, proportionally decrease with δ and proportionally increase with d. We ran a step-wise regression with two-factors (i.e., products) of p^{-1}, δ and d on the collective set of 477,120 vehicles in our simulation. The step-wise regression model yielded $F(p, \delta, d) = \beta_0^F + \beta_1^F dp^{-1} + \beta_2^F p^{-1} + \beta_3^F d + \beta_4^F \delta$ and estimated the parameter values to be $\beta_0^F = 13.94996$, $\beta_1^F = 40.97261$, $\beta_2^F = 418.88514$, $\beta_3^F = 0.14887$, and $\beta_4^F = -1.91644$ based on the given data. All coefficient values were found statistically significant at the 0.0001 level. Also, r^2 was 0.9959, indicating practically all variability in charging duration is explained by the estimated $F(p, \delta, d)$ function.

Energy demand and arrival SOC distributions are given among inputs of the simulation model from EVI-Pro. Incorporating their respective distributions, we obtain the expected value of charging duration as follows:

$$\begin{aligned} E[t_c] &= E[F(p)] \\ &= \beta_0^F + \beta_1^F E[d] p^{-1} + \beta_2^F p^{-1} + \beta_3^F E[d] + \beta_4^F E[\delta] \\ &= \left[\beta_0^F + \beta_3^F E[d] + \beta_4^F E[\delta]\right] + \left[\beta_1^F E[d] + \beta_2^F\right] p^{-1} \\ &= \beta_0^{F'} + \beta_1^{F'} p^{-1} \end{aligned} \quad (1)$$

Here, $\beta_0^{F'} = \beta_0^F + \beta_3^F E[d] + \beta_4^F E[\delta]$ and $\beta_1^{F'} = \beta_1^F E[d] + \beta_2^F$. In our data set, these two parameter values were calculated as $\beta_0^{F'} = 9.41316$ and $\beta_1^{F'} = 1767.97909$. In addition, we conducted a simple linear regression analysis between p_1 and the actual average charging durations. Each actual duration (for a given p value) is averaged over $142 \times 28 \times 10 \times 4 = 159,040$ vehicles. The regression analysis resulted in $r^2 = 0.9880$, showing a very strong relationship even for only 3 observed p values.

Table III: Probability of queuing duration for three stations at different times of day (%).

Time	0-5 min			5-10 min			10-15 min			15-20 min			20-25 min			>25 min		
Inverval	St. 1	St. 2	St. 3	St. 1	St. 2	St. 3	St. 1	St. 2	St. 3	St. 1	St. 2	St. 3	St. 1	St. 2	St. 3	St. 1	St. 2	St. 3
00:00-02:00	100	100	0	0	0	0	0	0	0	0	0	0	0	0	0	0	0	0
02:00-04:00	100	100	0	0	0	0	0	0	0	0	0	0	0	0	0	0	0	0
04:00-06:00	100	100	84.16	0	0	2.97	0	0	0	0	0	0.99	0	0	0	0	0	10.89
06:00-08:00	100	100	78.19	0	0	2.13	0	0	0.53	0	0	1.06	0	0	2.13	0	0	15.43
08:00-10:00	100	99.07	56.35	0	0.28	1.11	0	0.47	4.45	0	0.19	2.67	0	0	3.12	0	0	28.29
10:00-12:00	99.78	98.07	43.05	0.21	0.87	2.51	0.01	0.75	2.51	0	0.25	3.18	0	0.06	4.52	0	0	34.34
12:00-14:00	99.05	96.57	36.48	0.89	1.77	3.09	0.06	1.05	3.81	0	0.39	2.18	0	0.22	2.54	0	0	37.75
14:00-16:00	99.67	95.89	46.04	0.31	2.15	4.46	0.01	0.95	3.85	0	0.7	4.26	0	0.19	3.85	0	0.13	27.18
16:00-28:00	99.84	99.47	47.23	0.12	0.35	2.11	0.04	0.18	3.43	0	0	5.28	0	0	1.85	0	0	29.02
18:00-20:00	100	99.17	61.01	0	0	1.38	0	0.55	3.21	0	0	3.21	0	0.28	4.59	0	0	22.48
20:00-22:00	100	100	84.42	0	0	1.30	0	0	0	0	0	2.60	0	0	2.60	0	0	5.19
22:00-24:00	100	100	100	0	0	0	0	0	0	0	0	0	0	0	0	0	0	0

B. Estimating the waiting time in the queue

The queueing system underlying the modeled charging station operation is complicated by (i) time-dependent arrivals, (ii) a general service time distribution, and (iii) multiple servers (i.e., ports), in order of their importance in increasing the complexity.

Arrival time distribution is time-dependent, and there is much fluctuation between arrivals during peak and non-peak hours. Our approach in defining waiting time (W_q) focuses on the peak hours[1] (i.e., worst case), hence customers arriving in non-peak hours can expect to get their service after significantly shorter waiting.

We assume inter-arrival times are exponentially distributed, as is common in numerous queueing applications. The queueing theory gives us a useful baseline, however it falls short of giving us a closed-form expression to estimate average waiting (in-queue) time. Furthermore, our focus in this study is on the average waiting time during peak hours. We bridge the gap between the queueing theory and our needs with analytics as follows.

The best closed-form estimate of W_q we can use from the queueing theory is from the $M/M/c$ model, which assumes exponential inter-arrival and service times, and multiple ($c > 1$) servers [26, Section 3.3]. In our application, each port is a server, hence we replace c by n in the formulation. We denote this estimate by Ω_q and express it as follows:

$$\Omega_q = \frac{\frac{(\lambda/\mu)^n}{n!(n\mu-\lambda)^2}}{\sum_{i=0}^{n-1}\frac{(\lambda/\mu)^i}{i!}+\sum_{i=n}^{\infty}\frac{(\lambda/\mu)^i}{n^{i-n}n!}} \tag{2}$$

Here, λ is the arrival rate in vehicles per minute, which is known a priori. On the other hand, μ is the service rate in vehicles per minute, which depends on the setup time and charging durations as follows.

$$\begin{aligned}\mu &= (s + E[t_c])^{-1} \\ &= \left(s + \beta_0^{F'} + \beta_1^{F'} p^{-1}\right)^{-1}\end{aligned} \tag{3}$$

where s is taken as 5 min. Plugging (3) into (2), we get the following closed form equation:

$$\Omega_q = \frac{\frac{\left(\lambda\left(s+\beta_0^{F'}+\beta_1^{F'}p^{-1}\right)\right)^n}{n!\left(\frac{n}{\left(s+\beta_0^{F'}+\beta_1^{F'}p^{-1}\right)}-\lambda\right)^2}}{\sum_{i=0}^{n-1}\frac{\left(\lambda\left(s+\beta_0^{F'}+\beta_1^{F'}p^{-1}\right)\right)^i}{i!}+\sum_{i=n}^{\infty}\frac{\left(\lambda\left(s+\beta_0^{F'}+\beta_1^{F'}p^{-1}\right)\right)^i}{n^{i-n}n!}} \tag{4}$$

We hypothesize that the expected queue time is a function of n and p, i.e., $E[W_q] = G(n,p)$. We use Ω_q, which is a a closed-form nonlinear function of n and p itself, as a factor in estimating the G function. We also use the inverses of μ and n as factors. The smaller the inverse of the service rate or the number of ports, the shorter we expect vehicles to wait in queue. We again performed a step-wise regression based on two-factors of Ω_q, n^{-1} and μ^{-1} to estimate the G function. Based on the 12 observations from our simulations, the best estimate of the G function is the following:

$$G(n,p) = \beta_0^G + \beta_1^G\Omega_q + \beta_2^G\Omega_q n^{-1} + \beta_3^G(n\mu)^{-1} \tag{5}$$

Here, the parameter values were estimated as $\beta_0^G = -21.20508$, $\beta_1^G = 134.44303$, $\beta_2^G = -947.71254$, and $\beta_3^G = 6.62322$. In the model, all coefficient values were found significant at the 0.01 level. Also, $r^2 = 0.9968$, which indicates a very strong relationship.

Plugging the service rate estimation (3) into the waiting time estimation (5), we get the following expression:

$$\begin{aligned}G(n,p) &= \beta_0^G+\beta_1^G\Omega_q+\beta_2^G\Omega_q n^{-1}+\beta_3^G(n\mu)^{-1} \\ &= \beta_0^G+\beta_1^G\Omega_q+\beta_2^G\frac{\Omega_q}{n}+\beta_3^G\frac{\left(s+\beta_0^{F'}+\beta_1^{F'}p^{-1}\right)}{n} \\ &= \beta_0^G+\beta_1^G\Omega_q+\beta_2^G\frac{\Omega_q}{n}+\beta_3^G\left(s+\beta_0^{F'}\right)\frac{1}{n}+\beta_3^G\beta_1^{F'}\frac{1}{np} \\ &= \beta_0^G+\beta_1^G\Omega_q+\beta_2^G\frac{\Omega_q}{n}+\beta_3^{G'}\frac{1}{n}+\beta_4^{G'}\frac{1}{np}\end{aligned} \tag{6}$$

Here, $\beta_3^{G'} = \beta_3^G\left(s+\beta_0^{F'}\right)$ and $\beta_4^{G'} = \beta_3^G\beta_1^{F'}$. Recall that Ω_q is a function of n and p, and it is kept in equation (6) for sake of brevity in the formula.

C. Estimating the total cost

Both investment and operation costs can depend on the design criteria of a charging station. Investment costs include a fixed term f that may depend on factors such as location, but not the total station power, number of ports or the power of each port. We consider variable terms of investment costs

[1]the peak hours are designated as 10:00AM-4:00PM based on the field mobility data provided by EVI-Pro

in two parts: $\alpha(P)$ and $n\beta(p)$. Both α and β are assumed nonlinear functions that are monotonically non-decreasing and have diminishing returns in P and p, respectively, consistent with the cost function estimated in [27].

Operation costs depend largely on the energy consumption and the traffic going through the station. Pricing and other demand management tools can be utilized to assure that each additional vehicle charged in the station yields at least enough revenue to cover the operational costs it causes. Therefore, in the current work, we focus on analyzing the trade-offs between investment cost and customer satisfaction. Total investment cost (Z) is expressed as follows.

$$\text{Minimize } Z = f + \alpha(P) + n\beta(p) \tag{7}$$

V. Optimization of DCFC Station Capacity and Number of Ports

There is an inherent trade-off in cost vs. customer satisfaction. With increased competition among station operators, customer satisfaction becomes more important. Keeping costs low can mean sacrificing customer satisfaction, however it is necessary for the long term and for financial sustainability of any given station operator. In the case of a charging station, customer satisfaction can be measured via waiting time during peak hours.

The trade-off between total investment cost calculated using an example cost function and average waiting times during peak hours (W_q) is depicted in Figure 9a. The example cost function is $Z = -0.6699P^2 + 1919.4565P + n(-0.4145p^2 + 520.7421p)$, which approximates the costs reported in [27] for the case without solar panel or battery storage investment. The actual observations for every (n, p) combination are depicted by the blue diamonds and acquired using the developed DCFC model explained in Section III. The "expected" orange circles in the same figure are the estimates calculated via equation (6). The expected values are calculated for each even p value in the interval $[48, 72]$ kW, to display the trade-off in more detail. It is seen in the figure that the actual and expected values are very close together, and they both show a "frontier" in the quest to minimize both Z and W_q (for quality, or, customer satisfaction).

Figure 9b displays the efficient frontier consisting of select "expected" points from Figure 9a. More specifically, the efficient frontier contains only such solutions that can be ordered and then connected with line segments without leaving any solution, i.e., point, to the bottom-left side of any line segment. This definition also ensures that, the line segments are ordered from steepest to slightest when the points are ordered from left to right.

The decision maker can use the trade-off information conveyed in Figures 9a and 9b to select a solution in a number of ways. Firstly, a new objective function in the form of $\Omega = Z + \lambda W_q$ can be formulated. In this structure, λ is the relative penalty associated with increasing W_q by a minute compared to increasing Z by $\$1,000,000$. For each value of λ, a point on the efficient frontier is optimal, i.e., minimizes this objective function. Table IV shows which efficient solution is optimal for what values of λ. Note that λ intervals overlap, hence for some λ values there are two optimal solutions.

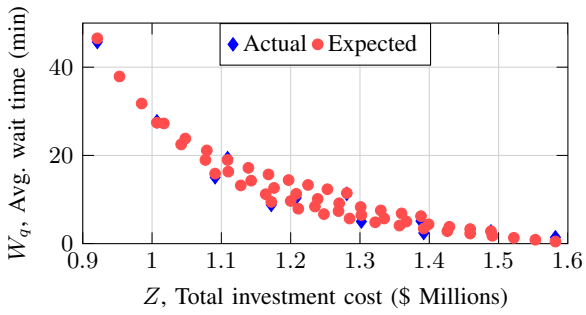

(a)

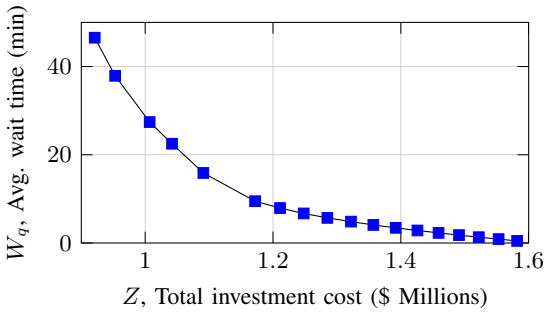

(b)

Figure 9: (a) Trade-off between Z and W_q and (b) Efficient frontier.

Table IV: Optimal efficient solution for slope (λ) values

λ	Z	W_q
$\leq$0.003769	0.921	46.534
$\geq$0.003769 AND $\leq$0.005179	0.953	37.895
$\geq$0.005179 AND $\leq$0.007090	1.007	27.412
$\geq$0.007090 AND $\leq$0.007389	1.042	22.495
$\geq$0.007389 AND $\leq$0.012596	1.091	15.877
$\geq$0.012596 AND $\leq$0.024882	1.172	9.473
$\geq$0.024882 AND $\leq$0.031049	1.211	7.918
$\geq$0.031049 AND $\leq$0.036985	1.248	6.698
$\geq$0.036985 AND $\leq$0.042517	1.285	5.696
$\geq$0.042517 AND $\leq$0.047588	1.322	4.844
$\geq$0.047588 AND $\leq$0.052212	1.357	4.099
$\geq$0.052212 AND $\leq$0.056434	1.392	3.436
$\geq$0.056434 AND $\leq$0.060304	1.426	2.837
$\geq$0.060304 AND $\leq$0.063869	1.459	2.290
$\geq$0.063869 AND $\leq$0.067167	1.491	1.786
$\geq$0.067167 AND $\leq$0.070227	1.522	1.318
$\geq$0.070227 AND $\leq$0.073069	1.553	0.883
$\geq$0.073069	1.582	0.476

Secondly, the decision maker may restrict either Z or W_q value via a new constraint and minimize the other (W_q or Z) among the remaining feasible efficient solutions. For example, a budget constraint may place an upper limit $\overline{Z}$ as depicted in Fig. 10a. If $Z \leq 1.3$ is imposed as shown in the figure, then $(Z = 1.285, W_q = 5.696)$ emerges as the optimal solution. Similarly, customer expectations may impose an upper limit on W_q as shown in Fig. 10b. For $W_q \leq 10$ shown in the figure, $(Z = 1.172, W_q = 9.473)$ is the resulting optimal solution.

The decision maker can also simply make his or her decision by simply observing the trade-off shown in Figure 9a. As long as the chosen solution is not dominated by another solution, i.e., there is no other solution with both smaller P and smaller W_q, then the chosen solution can be a good choice even if it is not on the efficient frontier. For example, $(Z = 1.128, W_q = 13.194)$ may appear very attractive to the decision maker in his/her evaluation even if it's slightly on the upper-right side of the efficient frontier. Multi-criteria decision making is complex even for only two criteria. We refer the

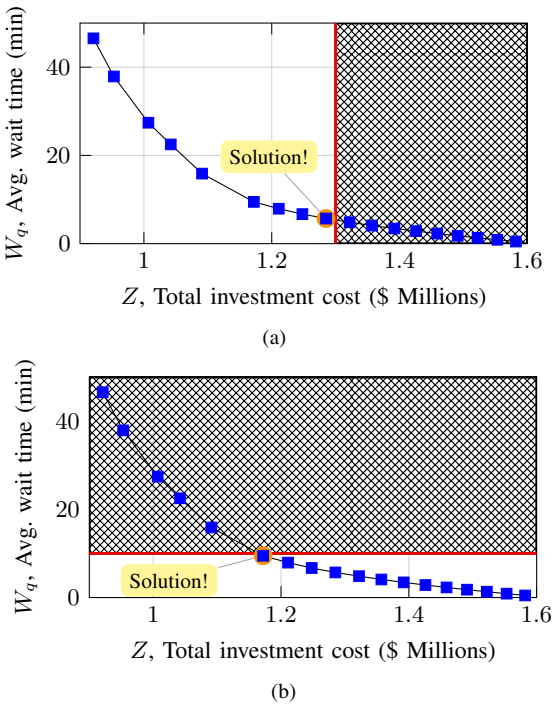

Figure 10: Minimizing (a) W_q for constrained P and (b) Minimizing P for constrained W_q.

reader to [28] for further reading on the approaches presented here and more.

VI. Conclusions and Future Work

In this work, we developed a DCFC station model and analyzed three different DCFC stations using charging and mobility data acquired from EVI-Pro. The model ran a thorough analysis on DCFC station operation to understand statistical metrics such as peak demand power, customer service quality, and port utilization. While the increased station power capacity and number of ports result in a higher peak demand power, it is very dependent on EV charge acceptance.

Further, increasing port number increases customer QoS but decreases port utilization. As an example, an 1,800 kW, 12-port DCFC resulted in a 33.7% peak loading and 30.8% port utilization. The probability of waiting more than five minutes in the queue at this station is at worst 0.95% during a day. We analyzed this relationship in greater detail with the use of the queueing theory and data analytics, and obtained a series of closed-form mathematical expressions to estimate queue time. We further explored the optimization of DCFC station power in a bi-objective model through the trade-off between cost and customer satisfaction. We showed increasing the number of ports for a given DCFC station power decreases waiting time.

Queueing theory is very useful in estimating waiting times, however it is also limiting due to its inherent mathematical complexity. In our present analysis, we focused our attention to homogeneous electric vehicle populations. Extension of the present work to heterogeneous populations emerges as a potential future research direction. Optimization of a DCFC station is complicated by factors such as space limitations, the current charge technology and the uncertainty regarding both the demand and technology development. For example, designing optimal control policies for a limited-capacity (P) station to serve a heterogeneous population of vehicles needs to be addressed.

Another possible future research direction is to integrate this analytical framework with empirical findings regarding customer behavior in order to optimize station design for the whole ecosystem. For example, customers may be impatient, i.e., they may show balking and/or reneging behaviors, which can be captured in the same framework. The extent of changes in the model under such impatience can be explored in a future extension of this study. Also, some customers may be concerned with the total (waiting plus charging) time in the system, more so than the waiting time alone. Such a change in the cost vs. QoS trade-off is expected to shift the optimal solution towards fewer faster ports. A more complex system design incorporating multi-level prioritization of ports and/or customers, possibly with different prices may be studied to quantify the effects as well as to jointly optimize for multiple stakeholders at the same time.

References

[1] M. C. Kisacikoglu, A. Bedir, B. Ozpineci, and L. M. Tolbert, "PHEV-EV charger technology assessment with an emphasis on V2G operation," Oak Ridge Nat. Lab., Tech. Rep. ORNL/TM-2010/221, Mar. 2012.

[2] D. Berjoza and I. Jurgena, "Analysis of distribution of electric vehicle charging stations in the Baltic," *Eng. Rural Develop.*, vol. 14, no. January, pp. 258–264, 2015.

[3] I. Zenginis, J. S. Vardakas, N. Zorba, and C. V. Verikoukis, "Analysis and quality of service evaluation of a fast charging station for electric vehicles," *Energy*, vol. 112, pp. 669–678, 2016.

[4] P. Fan, B. Sainbayar, and S. Ren, "Operation analysis of fast charging stations with energy demand control of electric vehicles," *IEEE Trans. Smart Grid*, vol. 6, no. 4, pp. 1819–1826, 2015.

[5] K. Yunus, H. Z. De La Parra, and M. Reza, "Distribution grid impact of plug-in electric vehicles charging at fast charging stations using stochastic charging model," in *Proc. 14th Eur. Conf. Power Electron. Appl.*, Aug 2011.

[6] E. Akhavan-Rezai, M. F. Shaaban, E. F. El-Saadany, and A. Zidan, "Uncoordinated charging impacts of electric vehicles on electric distribution grids: Normal and fast charging comparison," in *IEEE Power Energy Soc. General Meeting*, July 2012.

[7] Q. Yang, S. Sun, S. Deng, Q. Zhao, and M. Zhou, "Optimal sizing of PEV fast charging stations with markovian demand characterization," *IEEE Trans. Smart Grid*, in press.

[8] C. Farkas and M. Telek, "Capacity planning of electric car charging station based on discrete time observations and map(2)/g/c queue," *Period. Polytech., Electr. Eng. Comput. Sci.*, vol. 62, no. 3, pp. 82–89, 2018.

[9] E. Wood, S. Raghavan, C. Rames, J. Eichman, and M. Melaina, "Regional charging infrastructure for plug-in electric Massachusetts," Nat. Renewable Energy Lab. (NREL), Golden, CO, Tech. Rep. DOE/GO-102016-4922, 2017.

[10] E. Wood, C. Rames, M. Muratori, S. Raghavan, and M. Melaina, "National plug-in electric vehicle infrastructure analysis," Nat. Renewable Energy Lab. (NREL), Golden, CO, Tech. Rep. DOE/GO-102017-5040, 2017.

[11] U.S. Dept. Transport., "Smart city challenge," https://www.transportation.gov/smartcity, [Online; accessed 09-Aug-2018].

[12] Alternative Fuels Data Center, "Electric vehicle infrastructure projection tool (evi-pro) lite," https://www.afdc.energy.gov/evi-pro-lite, [Online; accessed 09-Aug-2018].

[13] H. Zhang, Z. Hu, Z. Xu, and Y. Song, "Optimal planning of PEV charging station with single output multiple cables charging spots," *IEEE Trans. Smart Grid*, vol. 8, no. 5, pp. 2119–2128, 2017.

[14] Y. Xiang, J. Liu, R. Li, F. Li, C. Gu, and S. Tang, "Economic planning of electric vehicle charging stations considering traffic constraints and load profile templates," *Applied Energy*, vol. 178, pp. 647–659, 2016.

[15] J. Yang, J. Dong, and L. Hu, "A data-driven optimization-based approach for siting and sizing of electric taxi charging stations," *Transport. Research Part C: Emerging Tech.*, vol. 77, pp. 462–477, 2017.

[16] E. Wood, C. Rames, M. Muratori, S. Raghavan, and S. Young, "Charging electric vehicles in smart cities: An EVI-Pro analysis of columbus, ohio." Nat. Renewable Energy Lab. (NREL), Golden, CO, Tech. Rep. NREL/TP-5400-70367, 2017.

[17] INRIX, "INRIX: Intelligence that moves the world," http://inrix.com/about/, [Online; accessed 20-Nov-2017].

[18] Idaho Nat. Lab., "2013 Nissan Leaf: Advanced vehicle testing activity," https://avt.inl.gov/vehicle-button/2013-nissan-leaf, [Online; accessed 24-Nov-2017].

[19] General Motors, "Drive unit and battery at the heart of Chevrolet Bolt EV, press release," http://media.gm.com/media/cn/en/gm/news.detail.html/content/Pages/news/cn/en/2016/jan/0114_bolt-ev.html, [Online; accessed 24-Nov-2017].

[20] Nissan Motor Co., "Electric vehicle lithium-ion battery Nissan technological development activities," http://www.nissan-global.com/en/technology/overview/li_ion_ev.html, [Online; accessed 24-Nov-2017].

[21] R. Klein, N. A. Chaturvedi, J. Christensen, J. Ahmed, R. Findeisen, and A. Kojic, "Optimal charging strategies in lithium-ion battery," in *American Control Conf. (ACC)*, 2011, pp. 382–387.

[22] Y.-H. Liu, J.-H. Teng, and Y.-C. Lin, "Search for an optimal rapid charging pattern for lithium-ion batteries using ant colony system algorithm," *IEEE Trans. Ind. Electron.*, vol. 52, no. 5, pp. 1328–1336, 2005.

[23] G. Fitzgerald and C. Nelder, "EVgo fleet and tariff analysis," Rocky Mountain Inst., Tech. Rep., 2017.

[24] SAS. (2018) Sas 9.4 software. [Online; accessed 11-June-2018]. [Online]. Available: https://www.sas.com/en_us/software/sas9.html

[25] D. Anderson, D. Sweeney, T. Williams, J. Camm, and J. Cochran, *Statistics for Business & Economics*. Cengage Learning, 2016. [Online]. Available: https://books.google.com/books?id=6r0aCgAAQBAJ

[26] J. F. Shortle, J. M. Thompson, D. Gross, and C. M. Harris, *Fundamentals of queueing theory*. John Wiley & Sons, 2018, vol. 399.

[27] J. Francfort, S. Salisbury, J. Smart, T. Garetson, and D. Karner, "Considerations for corridor and community DC fast charging complex system design," Idaho Nat. Lab., Idaho Falls, Idaho, Tech. Rep. INL/EXT-17-40829, 2017.

[28] Y. Collette and P. Siarry, *Multiobjective optimization: principles and case studies*. Springer Science & Business Media, 2013.

Emin Ucer (S'18) received the B.S. degree in Electrical and Electronics Engineering from Hacettepe University, Ankara, Turkey, in 2015.

He worked as a Research Engineer in TUBITAK (Scientific and Technological Research Council of Turkey) in the Division of Guidance, Control, and Navigation between 2015-2016. He's been working as Research Assistant&Ph.D. student at the University of Alabama since January 2017. His research interests are power electronics, electric vehicles (EVs), EV-grid integration and control. He is also interested in machine learning and artificial intelligence based techniques and their applications.

Isil Koyuncu received the B.S. degree from Bilkent University in 2013 in Ankara, Turkey and the M.S. degree from Koc University in 2015 in Istanbul, Turkey, both in Industrial Engineering.

Currently, she is pursuing her Ph.D. in Operations Management at The University of Alabama since 2015. Her research focuses on sustainable operations in transportation, especially routing decisions of fleets consisting of electric vehicles using integer programming.

Mithat C. Kisacikoglu (S'04–M'14) received the B.S. degree from Istanbul Technical University, Istanbul, Turkey, in 2005; M.S. degree from the University of South Alabama, Mobile, AL, in 2007; and the Ph.D. degree from the University of Tennessee, Knoxville, TN, in 2013, all in electrical engineering.

He worked at National Renewable Energy Laboratory, Golden, CO as a research engineer between 2015-2016. He is currently an Assistant Professor in the Electrical and Computer Engineering at University of Alabama, Tuscaloosa, AL. His research interests include electric vehicles (EVs), EV-grid integration, renewable energy sources, and power electronics converters. Dr. Kisacikoglu is an Associate Editor of The IEEE TRANSACTIONS ON INDUSTRY APPLICATIONS and IEEE TRANSACTIONS ON VEHICULAR TECHNOLOGY.

Mesut Yavuz received his B.S. (Industrial Engineering) degree in 1999 and M.S. (Engineering Management) degree in 2001 both from Istanbul Technical University. He received his Ph.D. (Industrial & Systems Engineering) from the University of Florida in 2005.

He is currently an associate professor of Operations Management in Culverhouse College of Commerce and Business Administration. Upon teaching at the University of Florida and Shenandoah University for 9 years, Dr. Yavuz joined University of Alabama's Culverhouse School of Business in 2014. His research is in the broad areas of computational optimization, production & distribution scheduling and sustainable transportation. His research has been supported by government agencies as well as corporations, and has been published in journals including Manufacturing & Service Operations Management and Transportation Science.

Andrew Meintz received his B.S. and Ph.D. degrees in Electrical Engineering from the Missouri University of Science and Technology in 2007 and 2011, respectively.

He is currently a senior research engineer at National Renewable Energy Laboratory (NREL) in Electric Vehicle Grid Integration. Prior to joining NREL in 2014, he was a Battery Systems engineer at General Motors with work on lithium-ion batteries for electric vehicles. Andrew has experience focused on advanced electric vehicle systems including fuel cells, power electronics and battery systems from projects in both academia and industry.

Clément Rames received his Master's degree in Mechanical Engineering from the University of Bristol, UK in 2016.

He is currently a Sustainable Mobility Research Engineer exploring the energy-mobility nexus from a data-driven, human-centered perspective at the National Renewable Energy Lab since 2016. His research aims to accelerate the transition to a sustainable and equitable mobility ecosystem through electrification, sharing, and multimodality. He previously studied at University of Texas at Austin. He has authored several publications on the energy impacts and infrastructure needs of emerging mobility technologies, and the links between urban form, mobility choices and vehicle ownership. He received the US Department of Energy Vehicle Technologies Office Team Award for his work on a National Plug-in Electric Vehicle Infrastructure Analysis, as well as Society of Automotive Engineer's Outstanding Presentation Award for his Analysis of Fast Charging Station Network for Electrifying Ride-hailing Services.